ARTICLES

Journal of Semiconductors
(2022) 43, 082601
doi: 10.1088/1674-4926/43/8/082601

Interlocked MXene/rGO aerogel with excellent mechanical stability for a health-monitoring device

Shufang Zhao[1, 2], Wenhao Ran[1, 2], Lili Wang[1, 2, †], and Guozhen Shen[1, 2, 3, †]

[1]State Key Laboratory for Superlattices and Microstructures, Institute of Semiconductors, Chinese Academy of Sciences, Beijing 100083, China
[2]Center of Materials Science and Optoelectronic Engineering, University of Chinese Academy of Sciences, Beijing 100083, China
[3]School of Integrated Circuits and Electronics, Beijing Institute of Technology, Beijing 100081, China

Abstract: Two-dimensional (2D) materials have attracted considerable interest thanks to their unique electronic/physical–chemical characteristics and their potential for use in a large variety of sensing applications. However, few-layered nanosheets tend to agglomerate owing to van der Waals forces, which obstruct internal nanoscale transport channels, resulting in low electrochemical activity and restricting their use for sensing purposes. Here, a hybrid MXene/rGO aerogel with a three-dimensional (3D) interlocked network was fabricated via a freeze-drying method. The porous MXene/rGO aerogel has a lightweight and hierarchical porous architecture, which can be compressed and expanded several times without breaking. Additionally, a flexible pressure sensor that uses the aerogel as the sensitive layer has a wide response range of approximately 0–40 kPa and a considerable response within this range, averaging approximately 61.49 kPa^{-1}. The excellent sensing performance endows it with a broad range of applications, including human-computer interfaces and human health monitoring.

Key words: flexible electronic; MXene/rGO; interlocking structure; high performance; healthcare monitoring

Citation: S F Zhao, W H Ran, L L Wang, and G Z Shen, Interlocked MXene/rGO aerogel with excellent mechanical stability for a health-monitoring device[J]. *J. Semicond.*, 2022, 43(8), 082601. https://doi.org/10.1088/1674-4926/43/8/082601

1. Introduction

In recent years, a diverse range of applications in the field of electronic sensing has emerged thanks to the unique properties of two-dimensional materials (e.g., graphene[1], MXene[2], metal oxides[3], etc.). These applications include pressure sensors, image sensors, biosensors, temperature/humidity sensors, and gas sensors[4–6]. In particular, researchers are interested in flexible pressure sensors because of their potential use in wearable health monitoring devices[7–9], human-machine interfaces[10–12], and electronic skins[13–15]. Research has shifted in recent years to improving sensor performance. Especially, electron/ion transport is influenced by the internal microstructure of the sensors (e.g., nanopores and nanochannels), which affects the sensor's ability to detect environmental changes[16]. Therefore, it is vital to investigate the inner microstructure of these materials, as well as the internal transport behavior of the sensors. The study of the inner microstructure of these materials and the internal transport behavior of sensors is therefore essential.

Graphene is a two-dimensional carbon substance with exceptional mechanical, electrical, thermal, and optical properties[17], and is currently a research hotspot. However, it is prone to agglomeration, which results in the destruction of internal nanoscale transport channels and a reduction in electrochemical activity, which limits its application in biosensing[18]. As a result, it cannot be used in biosensing applications. Graphene exhibits high electrochemical activity as well as biocompatibility. In recent years, a new class of 2D metal carbides and nitrides, the so-called MXene, has attracted extensive attention due to their metallic conductivity, excellent mechanical properties, and large specific surface area. Aerogel is a porous material with nanostructures that contain a large amount of air, which has unique properties in mechanics, acoustics, thermals, optics and so on. This ultralight and compressible aerogel material also has broad application prospects in the field of flexible sensing due to its high porosity, excellent compressibility, and electrical conductivity. The electrostatic interactions between MXene materials, with high electrochemical activity and biocompatibility, and graphene result in the creation of two-dimensional (2D) composites with low self-stacking that have good electrochemical activity and which are biocompatible[19, 20]. The composite material has better conductivity and can effectively improve the sensitivity of the sensor as a sensitive layer of the pressure sensor. The stacking of layered materials can effectively expand the response range of the sensor. Incorporating 2D materials as nanohybrids is being extensively explored to find their synergistic effect on sensing performance[21, 22].

In this paper we show that freeze-dried hybrid MXene-rGO aerogels with porous three-dimensional (3D) interlocked networks can be used as active layers to fabricate flexible sensors that exhibit high sensing performance. In addition, we demonstrate that the sensitivity of the flexible sensors increased with an increase in the bending angle (0°–90°). Moreover, these devices also possess an excellent level of reproducibility (high repeatability); namely, the sensitivity, response time, and recovery time do not significantly change after a large number of cycles. These outstanding demonstra-

Correspondence to: L L Wang, liliwang@semi.ac.cn; G Z Shen, gzshen@bit.edu.cn
Received 14 JANUARY 2022; Revised 9 MARCH 2022.

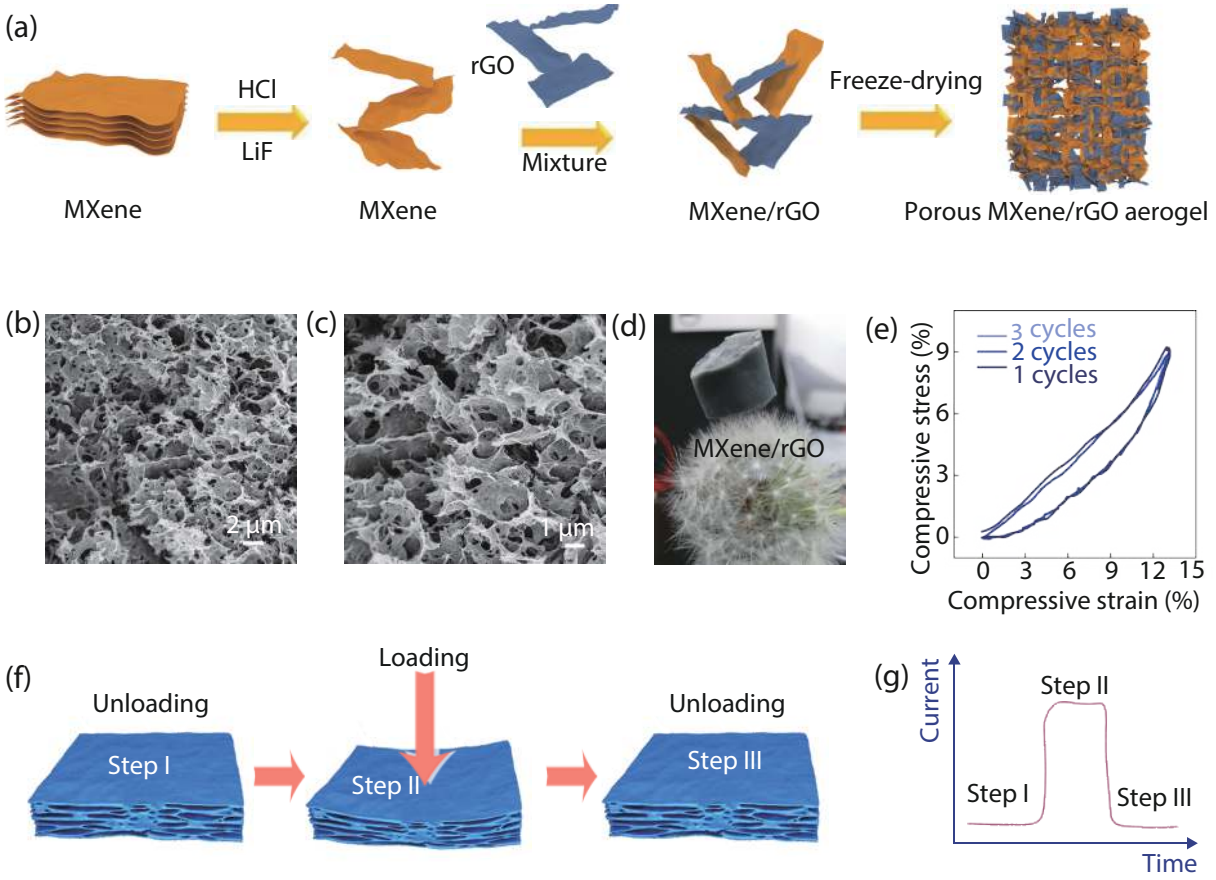

Fig. 1. (Color online) The characterization of the interlocked MXene/rGO aerogel composite. (a) Schematic illustration of the fabrication procedure of interlocked MXene/rGO aerogel. SEM images of interlocked MXene/rGO aerogel: (b) high magnification and (c) low magnification. (d) Optical image of interlocked MXene/rGO aerogel with lightweight feature placed on the dandelion. (e) Compressive stress-strain curves of the interlocked MXene/rGO aerogel at 12% strain under different cycles. (f) Structure change of interlocked MXene/rGO aerogel during the compression process and (g) the corresponding illustration of current change.

tions confirm the excellent performance of this interlocked material as a flexible and wearable sensor.

2. Methods

2.1. Preparation of interlocked MXene/rGO aerogel

$Ti_3C_2T_x$ was synthesized by selective etching of Al atoms from Ti_3AlC_2. Briefly, 4.8 g of lithium fluoride (LiF), 45 mL of hydrochloric acid (HCl) and 15 mL of deionized (DI) water were mixed by stirring. Then, 3 g of Ti_3AlC_2 was slowly added to the solution at 35 °C followed by stirring for 48 h. The as-obtained suspension was washed with deionized water via centrifugation at 3500 rpm until pH ⩾ 6. The above MXene nanosheets solution and rGO solution with mass ratio of 1 : 1 are mixed together using deionized water. Subsequently, as-obtained mixed solution based on MXene/rGO was poured into a tube and frozen for 30 min with liquid nitrogen. Finally, the MXene/rGO hybrid were freeze-dried in a lyophilizer for 48 h to fabricate 3D, interlocked MXene/rGO aerogels.

2.2. Sample characterization

The architecture of interlocked MXene/rGO aerogels was observed by scanning electron microscopy (SEM, Magellan 400). The dynamic pressure response and mechanical properties of an interlocked MXene/rGO aerogels-based flexible pressure sensor were tested using high-resolution micromechanical testing system (Instron E1000). Other pressure-sensitive properties were conducted using electrochemical work station (CHI 760E).

3. Results and discussion

3.1. Preparation of MXene/rGO aerogel

When rGO was added to the MXene nanosheet solution, an MXene/rGO aerogel with a 3D interlocked structure was formed via self-assembly and subsequent freeze-drying. Fig. 1(a) shows the preparation procedure of the interlocked MXene/rGO aerogel. Briefly, MXene nanosheets were created by etching a Ti_3AlC_2 precursor with HCl and LiF, followed by solution drying. A physical mixing procedure occurred between the charged MXene and rGO nanosheets. Upon combining the rGO with the MXene nanosheets, a thicker and more protective rGO layer was generated on the inner side of $Ti_3C_2T_x$. After freeze-drying, a 3D interlocked MXene/rGO hybrid aerogel was obtained.

The feasibility of freeze-drying for the preparation of the MXene/rGO aerogel was investigated using scanning electron microscopy (SEM). As shown in Fig. 1(b), the MXene and rGO nanosheets were extended and interlinked to form a 3D honeycomb-like network. Pores were created by the volatilization of water trapped between the MXene and rGO sheets after the aerogel was freeze-dried. According to a high-resolution SEM photograph, the pore sizes of these networks are in the range of several micrometers, which is simil-

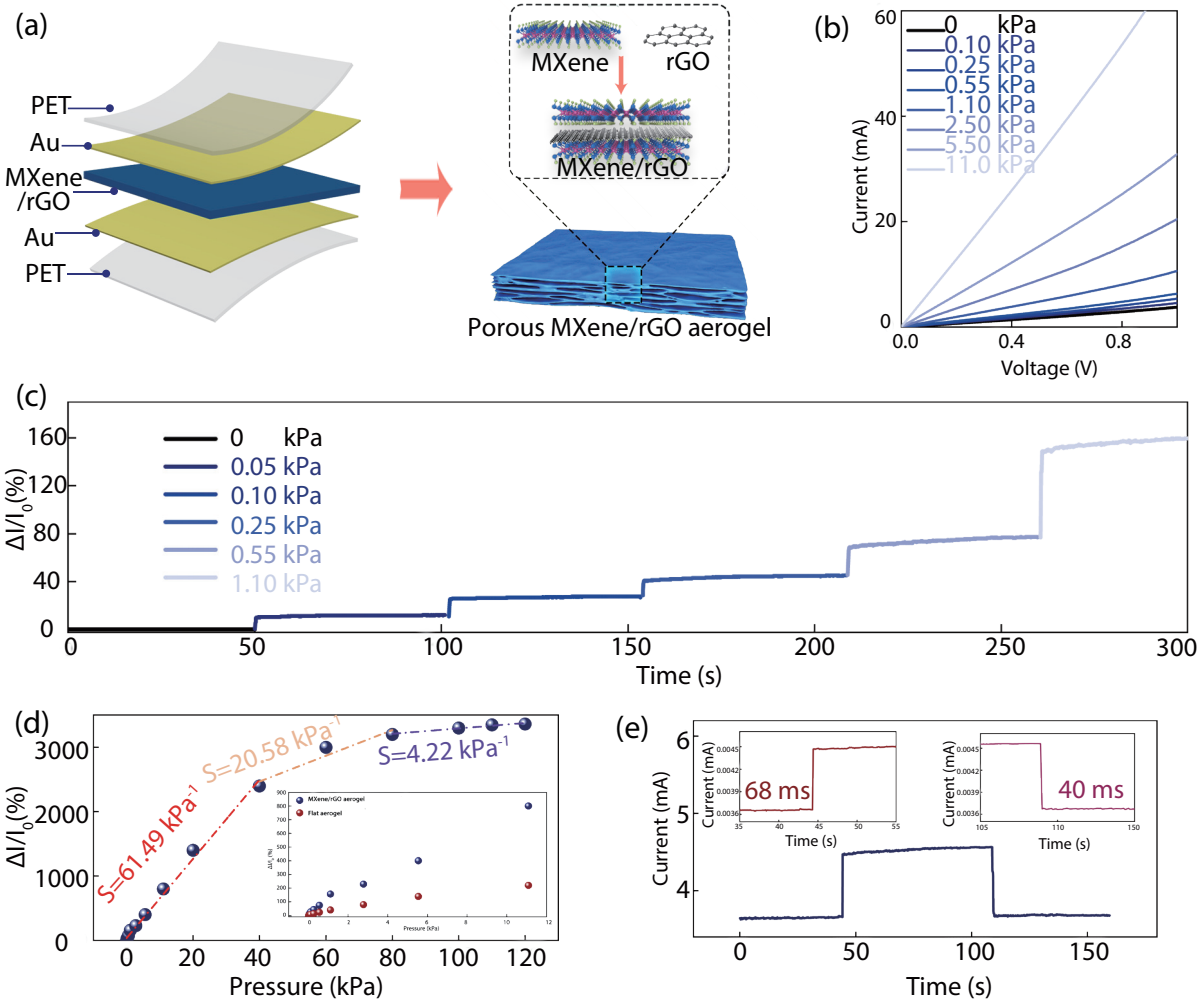

Fig. 2. (Color online) The sensing performance of the interlocked MXene/rGO aerogel-based pressure sensor. (a) Illustration of flexible pressure sensor. (b) The *I*–*V* curves of the flexible sensor. (c) Dynamic measurement of the sensor response with increased pressure from 0 to 1.1 kPa. (d) Sensitivity curves. Inset show the comparison of sensing properties of MXene/rGO aerogel and flat aerogel. (e) Current responses to loading/unloading 5.5 kPa on the sensor. The inserts give response time and recovery time of the sensor.

ar to a honeycomb-like network (Fig. 1(c)). Furthermore, the porous MXene/rGO aerogel is such a lightweight material that it can easily be held by a dandelion (Fig. 1(d)).

The elastic performance of the porous MXene/rGO aerogel was evaluated by testing the compressive loading and unloading curves with a maximum strain of 12%. When this strain was set, a much higher compressive stress of approximately 9.2 kPa could be observed. The stable and constant stress-strain curves in the 1st, 2nd, and 3rd cycles further confirmed the recoverability of the as-prepared MXene/rGO aerogel (Fig. 1(e)). The pressure-sensitive mechanism of the MXene/rGO aerogels was mainly related to the interlocking structure of the aerogels (Fig. 1(f)). Unlike planar films, MXene/rGO aerogels exhibit interlocking and porous structures. A porous structure can control the conductivity of aerogel materials. The change in the conductive channel depends on the applied external force. When an external pressure is applied, a small compression deformation of the porous MXene/rGO aerogel increases its internal conductive channel, as well as the current (Fig. 1(g)). During unloading, the aerogel reverts to its original shape and reduces the contact of the internal conductive channels, resulting in a decrease in the current (Fig. 1(g)).

3.2. Pressure sensing properties

Fig. 2(a) shows the structure of an interlocked MXene/rGO aerogel-based pressure sensor. We started by vacuum evaporating a gold electrode with a thickness of 50 nm onto a piece of polyethylene terephthalate film using a vacuum chamber. Then, using the previously developed interlocked MXene/rGO aerogel as an intermediary sensing layer, we designed a resistive pressure sensor that measures the current change at both ends of the aerogel under different pressures. The sensing performance of the interlocked MXene/RGO aerogel-based pressure sensor was studied using both static and dynamic mechanical pressure tests. The current–voltage curves of the aerogel-based pressure sensor under various static pressures ranging from 0 to 1.1 kPa are shown in Fig. 2(b). The current increases with an increase in the external force, which indicates that the sensitivity of the pressure sensor under static pressure is stable.

The corresponding dynamic sensitivity curves are shown in Fig. 2(c). The sensitivity of our pressure sensor was defined as $S = (\Delta I/I_0)/\Delta P$[10, 23–25], where ΔP denotes the change in the external force. ΔI denotes the relative change in the current and I_0 denotes the initial current. Fig. 2(d) diagrams the sensitivity of the pressure sensor under different pressure. In the

Table 1. Comparison of pressure sensor performance.

Device	Sensitivity (kPa^{-1})	Pressure range (kPa)	τ_{rise} (ms)	T_{decay} (ms)	Ref.
MXene/rGO	61.49	0–40	68	40	Our work
MXene/ANFs	6.75	–	320	98	[26]
Carbon nanotubes (CNTs)/graphene/waterborne polyurethane (WPU)/ cellulose nanocrystal (CNC) composite aerogels (CNTs/graphene/WC)	0.25	0.112–10	120		[27]
MXene/reduced graphene oxide (MX/rGO)	22.56	0.115–0.97	243	231	[24]
Graphene/biomass aerogels	13.89	<12	120	840	[28]
Polyimide (PI)/reduced graphene oxide (rGO) aerogel	1.33	<20	60	70	[29]

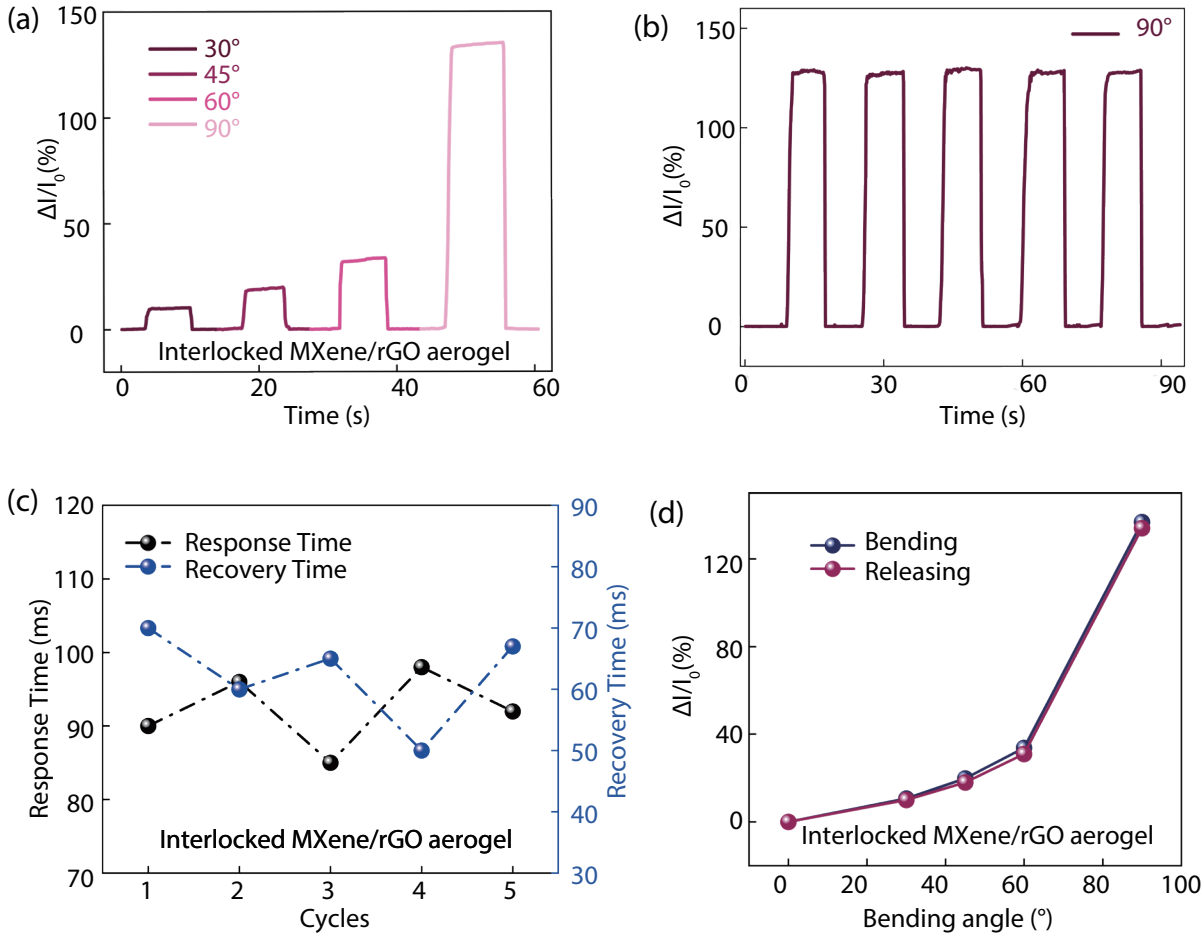

Fig. 3. (Color online) Sensing-performance of the interlocked MXene/rGO aerogel-based pressure sensor at different bending states. (a) The *I*–*T* curve with the bending angle increased from 30° to 90°. (b) The real-time *I*–*T* curve of the sensor in the 90° repeated bending-straightening process. (c) Response and recovery time under different cycles. (d) The bending stability test of the sensor under bending and releasing state.

pressure range of 0–40 kPa, the sensitivity of the flexible pressure sensor can reach 61.49 kPa^{-1}, which is much higher than that of conventional pressure sensors in the same range of values. When the pressure exceeds 40 kPa, the increase in sensitivity began to slow down and approaches saturation at 110 kPa with a sensitivity close to 4.22 kPa^{-1}. According to this study, our aerogel pressure sensors outperformed the other pressure sensors in terms of performance. The porous structure of the material is responsible for the reported enhanced pressure sensitivity levels.

We also compared the sensitivity of the flat aerogel pressure sensor and the MXene/rGO aerogel pressure sensor, and the results are shown in the inset of Fig. 2(d). As a result, the sensitivity of MXene/rGO aerogel-based pressure sensor is higher than flat aerogels-based pressure sensor. Fig. 2(e) shows another key parameter of the flexible device-response/recovery time; that is, from the current–time (*I*–*T*) amplification curve of the flexible device based on the interlocked MXene/rGO aerogel, the device has a faster response and recovery time (68 and 40 ms, respectively). These features correspond to the response and recovery time of the human skin (40–50 ms). Rapid response and recovery (without hysteresis) can ensure the timely perception of external forces by flexible devices and increase recognition efficiency. Furthermore, we compare the performance of the pressure sensor with the existing research results, and the results are shown in Table 1[24, 26–29]. Our pressure sensor has great advantages in terms of sensitivity, response range, response time and other performance.

To further study the mechanical stability of the inter-

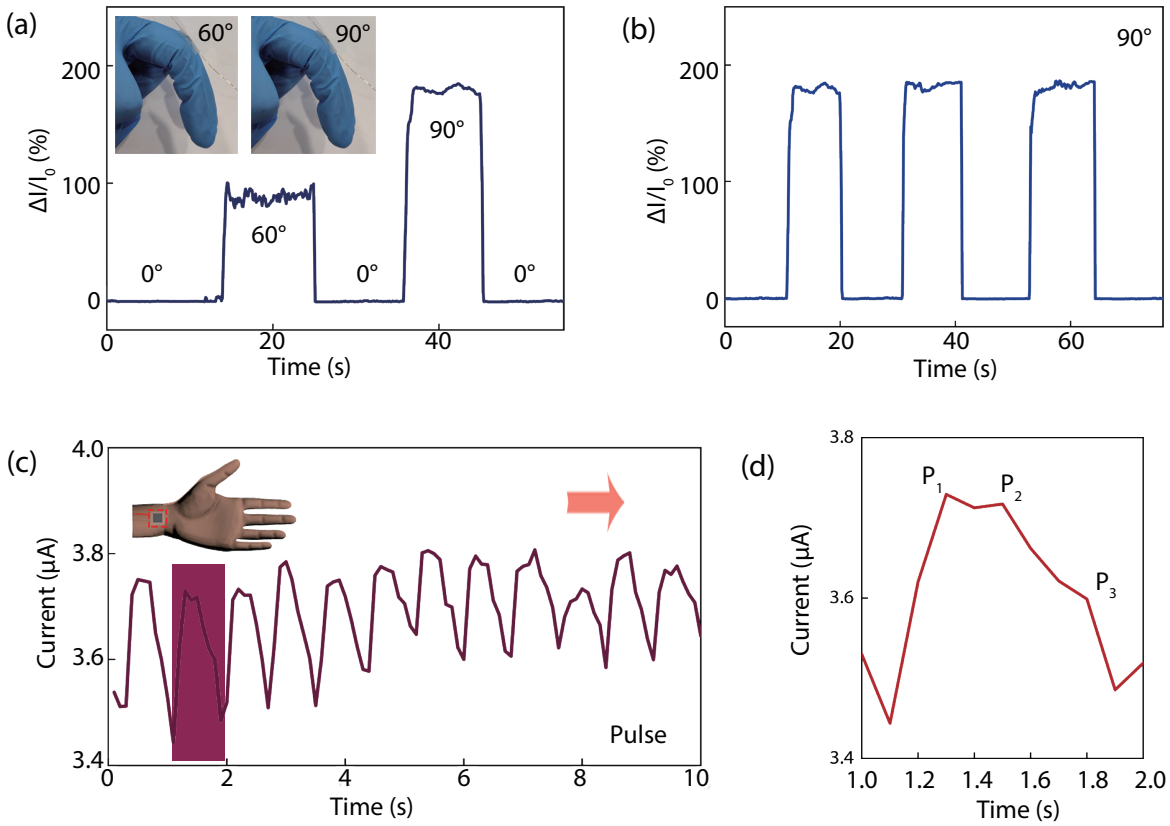

Fig. 4. (Color online) MXene/rGO aerogel-based pressure sensor as a wearable device for health monitoring. (a) The pressure-sensitive response to the bending motion of a forefinger (inset: photograph of the device fastened to back of a forefinger with different bending angles). (b) Three cycles of bending the finger at 90°. (c) Human pulse (inset: photograph of the device placed onto a wrist). (d) The enlarged waveform of one of the pulses in (c).

locked MXene/rGO aerogel-based pressure sensor, we tested the bending properties of the device at various angles (Fig. 3(a)). The pressure–sensitive response of the device increased with the extension of the bending angle. The change in sensitivity under bending deformation was studied at a bending angle of 90° (Fig. 3(b)). After five cycles, the pressure-sensitive response of the device was maintained at approximately 120. The interlocked aerogels exhibited high sensitivity and good cycling stability. At a bending angle of 90°, the pressure-sensitive response was approximately 120 and recovered to its initial value when released. Moreover, each corresponding cycle shows good response and recovery characteristics (Fig. 3(c)). Fig. 3(d) displays the sensor sensitivity under different bending angles (the bending angle started at $\theta = 0°$, and the gradient increased to 90° and then returned to 0° at a rate of 30°). This indicates the good mechanical stability of the flexible sensor, which retained the same level of pressure-sensitive response throughout the bending angle test.

3.3. Health monitoring

Owing to its supercompressibility, elasticity, fatigue resistance, bendability, and ultrahigh sensitivity, the interlocked MXene/rGO aerogel-based flexible pressure sensor offers a wide range of applications in wearable sectors. Based on the research results, our sensors accurately identified a variety of stimuli across a wide range of pressures, including finger joint motion and wrist pulses. As shown in Fig. 4(a), the output current increased with the bending angle of the index finger, and the amplitude of the output current increased with the bending degree of the index finger. Here, the index finger has a bend angle of 60°, and the pressure-sensitive response value is approximately 91. Furthermore, the repeatability of the device was demonstrated by bending the index finger at 90° three times in a row, while retaining a current response of approximately 170 (Fig. 4(b)).

Blood pressure readings collected from the wrist could provide vital and useful information about an individual's physical and mental well-being. Examples of such disorders include cardiovascular disease, which is related to the shape of the wrist pulse waveform. Thus, by monitoring the radial artery in the wrist, the sensor may be able to collect information regarding human pulses and other vital signs. As depicted in Fig. 4(c), the comparable pulse frequency was approximately 75 beat/min. Meanwhile, Fig. 4(c) depicts a pulse waveform with three distinct peaks: P_1 represents the percussion wave, P_2 the tidal wave, and P_3 the diastolic wave. Fig. 4(d) depicts the signs and symptoms of various cardiovascular disorders. Because the wrist pulse waveform can be used to predict a variety of cardiovascular diseases, our sensors may have a future in real-time health monitoring. Based on these initial findings, it appears that this flexible pressure sensor could find applications in several scenarios requiring reliable detection over a wide pressure range, such as wearable medical electronics and prosthetics[30–33].

4. Conclusion

In summary, the combination of MXene nanosheets with rGO resulted in a compressible and elastic MXene-derived aerogel with excellent mechanical properties and good flexibility.

Owing to good 3D interlocked structure of MXene/rGO aerogel, the sensor exhibits a good sensitivity of 61.49 kPa^{-1} throughout a broad linear response range of 0–40 kPa, fast response time (68 ms) and cycling stability. In addition, the aerogel-based sensor exhibits a high degree of linearity over a wide range of pressures and temperatures. Consequently, the pressure sensor was able to detect eight subtle, low-, and medium-level pressures, such as those produced by a human heartbeat or finger movement. These properties make aerogels potential candidates for use in pressure/strain sensors and wearable devices. Because of its higher performance and ease of fabrication, the proposed sensor may prove to be a viable option for use in artificial intelligence and smart medical devices in the future.

Acknowledgements

The authors sincerely acknowledge financial support from the National Natural Science Foundation of China (NSFC Grant No. 61625404, 61888102, 62174152), Young Elite Scientists Sponsorship Program by CAST (2018QNRC001), the Strategic Priority Program of the Chinese Academy of Sciences, Grant No XDA16021100, and the Science and Technology Development Plan of Jilin Province (20210101168JC).

References

[1] Cao M, Su J, Fan S, et al. Wearable piezoresistive pressure sensors based on 3D graphene. Chem Eng J, 2021, 406, 126777

[2] Jin X, Li L, Zhao S, et al. Assessment of occlusal force and local gas release using degradable bacterial cellulose/$Ti_3C_2T_x$ MXene bioaerogel for oral healthcare. ACS Nano, 2021, 15, 18385

[3] Wang L, Chen S, Li W, et al. Grain-boundary-induced drastic sensing performance enhancement of polycrystalline-microwire printed gas sensors. Adv Mater, 2019, 31, 1804583

[4] Wu J, Huang D, Ye Y, et al. Theoretical study of a group IV p–i–n photodetector with a flat and broad response for visible and infrared detection. J Semicond, 2020, 41, 122402

[5] Zhong B, Jiang K, Wang L, et al. Wearable sweat loss measuring devices: From the role of sweat loss to advanced mechanisms and designs. Adv Sci, 2022, 9, 2103257

[6] Geng R, Gong Y. High performance active image sensor pixel design with circular structure oxide TFT. J Semicond, 2019, 40, 022402

[7] Zhao S, Ran W, Wang D, et al. 3D dielectric layer enabled highly sensitive capacitive pressure sensors for wearable electronics. ACS Appl Mater Interfaces, 2020, 12, 32023

[8] Mak P I. Lab-on-COS-an in-vitro diagnostic (IVD) tool for a healthier society. J Semicond, 2020, 41, 110301

[9] Zhang Z, Chen C, Fei T, et al. Wireless communication and wireless power transfer system for implantable medical device. J Semicond, 2020, 41, 102403

[10] Chen T, Zhang S H, Lin Q H, et al. Highly sensitive and wide-detection range pressure sensor constructed on a hierarchical-structured conductive fabric as a human-machine interface. Nanoscale, 2020, 12, 21271

[11] Wang L, Jiang K, Shen G. A perspective on flexible sensors in developing diagnostic devices. Appl Phys Lett, 2022, 119, 150501

[12] Li L, Wang D, Zhang D, et al. Near-infrared light triggered self-powered mechano-optical communication system using wearable photodetector textile. Adv Funct Mater, 2021, 31, 2104782

[13] Kang K, Jung H, An S, et al. Skin-like transparent polymer-hydrogel hybrid pressure sensor with pyramid microstructures. Polymers, 2021, 13, 3272

[14] Qi K, Zhou Y, Ou K, et al. Weavable and stretchable piezoresistive carbon nanotubes-embedded nanofiber sensing yarns for highly sensitive and multimodal wearable textile sensor. Carbon, 2020, 170, 464

[15] Wang G, Wang Z, Wu Y, et al. A robust stretchable pressure sensor for electronic skins. Org Electron, 2020, 86, 105926

[16] Torad N L, Ding B, El-Said WA, et al. Mof-derived hybrid nanoarchitectured carbons for gas discrimination of volatile aromatic hydrocarbons. Carbon, 2020, 168, 55

[17] Bai H, Li C, Shi G. Functional composite materials based on chemically converted graphene. Adv Mater, 2011, 23, 1089

[18] Sun J, Du S. Application of graphene derivatives and their nanocomposites in tribology and lubrication: A review. RSC Adv, 2019, 9, 40642

[19] Pan H. Ultra-high electrochemical catalytic activity of MXenes. Sci Rep, 2016, 6, 32531

[20] Zhao L, Wang Z, Li Y, et al. Designed synthesis of chlorine and nitrogen co-doped Ti_3C_2 MXene quantum dots and their outstanding hydroxyl radical scavenging properties. J Mater Sci Technol, 2021, 78, 30

[21] Kamath K, Adepu V, Mattela V, et al. Development of $Ti_3C_2T_x/MoS_{2x}Se_{2(1-x)}$ nanohybrid multilayer structures for piezoresistive mechanical transduction. ACS Appl Electron Mater, 2021, 3, 4091

[22] Sun J, Du H, Chen Z, et al. MXene quantum dot within natural 3D watermelon peel matrix for biocompatible flexible sensing platform. Nano Res, 2022, 15, 3653

[23] Gong S, Schwalb W, Wang Y, et al. A wearable and highly sensitive pressure sensor with ultrathin gold nanowires. Nat Commun, 2014, 5, 3132

[24] Ma Y, Yue Y, Zhang H, et al. 3D synergistical MXene/reduced graphene oxide aerogel for a piezoresistive sensor. ACS Nano, 2018, 12, 3209

[25] Tian Y, Han J, Yang J, et al. A highly sensitive graphene aerogel pressure sensor inspired by fluffy spider leg. Adv Mater Interfaces, 2021, 8, 2100511

[26] Wang L, Zhang M, Yang B, et al. Thermally stable, light-weight, and robust aramid nanofibers/Ti_3AlC_2 MXene composite aerogel for sensitive pressure sensor. ACS Nano, 2020, 8, 10633

[27] Zhai J, Zhang Y, Cui C, et al. Flexible waterborne polyurethane/cellulose nanocrystal composite aerogels by integrating graphene and carbon nanotubes for a highly sensitive pressure sensor. ACS Sustain Chem Eng, 2021, 9, 14029

[28] Wei S, Qiu X, An J, et al. Highly sensitive, flexible, green synthesized graphene/biomass aerogels for pressure sensing application. Compos Sci Technol, 2021, 7, 20,108730

[29] Xu Q, X Chang, Zhu Z, et al. Flexible pressure sensors with high pressure sensitivity and low detection limit using a unique honeycomb-designed polyimide/reduced graphene oxide composite aerogel. RSC Adv, 2021, 11, 11760

[30] Wang D, Wang L, Shen G. Nanofiber/nanowires-based flexible and stretchable sensors. J Semicond, 2020, 41, 041605

[31] Wei S J. Reconfigurable computing: a promising microchip architecture for artificial intelligence. J Semicond, 2020, 41, 020301

[32] Wang K, Lou Z, Wang L, et al. Bioinspired interlocked structure-induced high deformability for two-dimensional titanium carbide (MXene)/natural microcapsule-based flexible pressure sensors. ACS Nano, 2019, 13, 9139

[33] Dong K, Wang Z L. Self-charging power textiles integrating energy harvesting triboelectric nanogenerators with energy storage batteries/supercapacitors. J Semicond, 2021, 42, 101601

Shufang Zhao is currently a Ph.D. candidate at the Institute of Semiconductors, Chinese Academy of Sciences. Her current scientific interests focus on the design and manufacture of flexible electronic skin and artificial nerve synapses, and investigation of their fundamental properties.

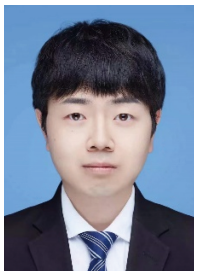

Wenhao Ran is currently a Ph.D. candidate at the Institute of Semiconductors, Chinese Academy of Sciences. His current scientific interests focus on the design and preparation of low- dimensional materials and their fundamental properties.

Lili Wang is a professor in the Institute of Semiconductors, Chinese Academy of Sciences, China. She earned her B.Sc. (2010) in chemistry and Ph.D. degree in microelectronics and solid state electronics from the Jilin University in 2014. Her current research interests focus on the flexible electronics based on biological materials, 2D materials and semiconductor, including pressure sensors, electronic-skin, biosensor, photodetectors and flexible energy storage and conversion devices.

Guozhen Shen received his B.Sc. degree (1999) in chemistry from Anhui Normal University and Ph.D. degree (2003) in chemistry from the University of Science and technology of China. He joined the Institute of Semiconductors, Chinese Academy of Sciences, as a Professor in 2013. He has published more than 200 papers with a publication H-factor of 57. His current research focuses on flexible electronics and printable electronics, including transistors, photodetectors, sensors and flexible energy storage and conversion devices.